JOURNAL OF MATERIALS SCIENCE 33 (1998) 1343–1348

Preparation of $Pb(Mg_{1/3}Nb_{2/3})O_3$–$Pb(Zn_{1/3}Nb_{2/3})O_3$ ceramics by the B-site precursor method and dielectric characteristics

MIN-CHUL CHAE, NAM-KYOUNG KIM, JEONG-JOO KIM, SANG-HEE CHO
Department of Inorganic Materials Engineering, Kyungpook National University, Taegu, South Korea 702-701
E-mail: nkkim@bh.kyungpook.ac.kr

Powders in the $Pb(Mg_{1/3}Nb_{2/3})O_3$–$Pb(Zn_{1/3}Nb_{2/3})O_3$ system, with a high perovskite yield, were prepared by a B-site precursor method. PbO was added to pre-reacted B-site components of $Mg_{1-x}Zn_xNb_2O_6$ solid solution, which was further calcined to form a perovskite structure. Perovskite phase contents and lattice parameters were obtained from X-ray analyses. Weak-field low-frequency dielectric constants and losses of sintered pellets were measured as functions of composition, temperature and frequency. Dielectric relaxation behaviours were investigated in terms of diffuseness coefficients. Microstructures were observed to correlate with other characteristics. © *1998 Chapman & Hall*

1. Introduction

With an increasing demand for electronic equipment of reduced size through high integration density, circuit devices and components are required to have small dimensions. Multilayer ceramic capacitors (MLCCs) have a high volumetric efficiency and meet the current trend of component miniaturization. In MLCC fabrication, however, internal electrodes must withstand the high firing temperatures of $BaTiO_3$-based materials during cofiring, which necessitates the use of noble metals, e.g., palladium. In order to reduce the high cost of electrodes by using less expensive silver-rich alloy, low-temperature-sinterable materials with high dielectric constants (20 000 or greater) have been intensively searched for and several of the lead-based mixed B-site cation perovskite compounds, e.g., $Pb(Fe_{1/2}Nb_{1/2})O_3$ (PFN), $Pb(Mg_{1/3}Nb_{2/3})O_3$ (PMN) and $Pb(Zn_{1/3}Nb_{2/3})O_3$ (PZN), satisfy the requirements. Currently, MLCCs fabricated with these perovskite materials are gradually replacing aluminium and tantalum electrolytic capacitors owing to the compact design, no polarity and high reliability.

In some of the Pb-containing complex perovskite materials, the magnitude of the dielectric constant peak decreases whilst the dielectric loss peak increases and the temperatures of both peaks increase with increasing frequency. Dielectric materials showing this kind of relaxation (or frequency dispersion) behaviour are called relaxor ferroelectrics. Dielectric relaxation was reported to originate from the compositional inhomogeneity, i.e., statistical distribution of competing B-site ions in the octahedral cage of an ABO_3 perovskite lattice [1, 2]. When the difference in valencies or sizes of the octahedral ions becomes large, the six-fold cations tend to order themselves in order to reduce or minimize electrostatic energy or lattice strain [3]. A diffuse phase transition (DPT) describes the nature of a dielectric constant spectrum with a relatively broad peak, in contrast with a classical sharp first-order transition of $BaTiO_3$ and $PbTiO_3$. The broadness of the dielectric constant peak is also typical characteristic of relaxor ferroelectrics.

A main feature of the dielectric properties of PMN is a frequency-dependent dielectric constant spectrum with a broad peak just below room temperature. The dielectric constant maxima and Curie temperatures of PMN ceramics [4, 5] and single-crystal PZN [5–7] were reported to be 18 000 and $-10\,^{\circ}C$, and 22 000 and $140\,^{\circ}C$, respectively. Potential applications of PMN (and modifications thereof) include MLCCs, piezoelectric transducers [8], actuators [9, 10] and pyroelectric bolometers [11]. The processing of PMN ceramics, especially designing novel reaction routes, has been widely studied in order to improve dielectric properties through increased perovskite phase yield. However, any attempts to synthesize PZN in the perovskite structure by a conventional calcining–mixed-oxide process (or one-step calcination method) under atmospheric pressure were reported to be unsuccessful. The reason behind this failure can be interpreted in terms of the fact that the Zn^{2+} ions are too large (7.4 nm [12]) to fit into the octahedral cage of the perovskite lattice. So far, perovskite PZN can only be prepared under a high pressure of 2.5 GPa [13], while a single-crystal form has been prepared by a flux-growth method [7, 14, 15].

This study is a part of an investigation of dielectric characteristics on the $Pb(Mg_{1/3}Ta_{2/3})O_3$ (PMT)–PMN–PZN system. Experiments on PMT–PMN have already been carried out and the results

were reported elsewhere [16]. The whole experiments were designed so as firstly to gain experience on the preparation of relaxor ceramics and secondly to obtain general data on the distribution of the dielectric constant maxima and Curie temperatures throughout the ternary composition diagram.

2. Experimental procedure

Starting materials were PbO (99.5% purity), MgO (99.9%), ZnO (99.8%) and Nb_2O_5 (99.9%). Compositions were selected from the system $Pb(Mg_{(1-x)/3}Zn_{x/3}Nb_{2/3})O_3$ ($(1-x)$PMN–xPZN), with x ranging from 0 to 1 at regular intervals of 0.2. A B-site precursor method [17, 18] (more inclusive and generic term for a so-called columbite process [19] or two-step calcination method) was adopted in the preparation of the perovskite powders. In order to maintain exact stoichiometry, the moisture contents of raw chemicals and synthesized B-site powders were measured and introduced into the batch calculations. B-site component oxides, $Mg_{1-x}Zn_xNb_2O_6$ ($(1-x)$MN–xZN) were prepared first by mixing all constituent oxides except for PbO, followed by drying, calcining at 1050–1150 °C for 2 h and examination using X-ray diffraction (XRD) in order to identify the phases formed. PbO was then added to the resultant precursors and the mixtures were calcined at 800–1050 °C to obtain powders of desired composition. The optimum calcination condition of perovskite-phase PMN was 800 °C, which increased with increasing PZN content. Double calcinations were carried out, if required, in order to enhance the yield of perovskite content.

For a sintering study, the calcined powders were mixed with a poly(vinyl alcohol)–water solution, granulated, pressed uniaxially into pellets (10 mm diameter and about 0.7 mm thick) and further compacted isostatically at 170 MPa. To prevent lead loss during firing, the pellets were then embedded in an atmosphere powder of identical composition and were sintered in a double-crucible set-up (sealed with $PbZrO_3$ powder [20]) for 1 h at 1050–1200 °C (with decreasing temperature as the composition became PZN rich), after a 1 h hold at 550 °C for binder burn-out. Optimum sintering conditions were determined by considering the phase yield and fired density throughout the composition range. Thus, sintered specimens were polished and geometrical densities were measured. The pellets were also analysed using XRD for phase examination. After gold sputtering on major faces of samples as electrodes, the dielectric constant and loss characteristics were measured on cooling in the temperature range from -150 to 180 °C, using a computer-interfaced impedance–gain phase analyser (HP 4194A) at 1 kHz, 10 kHz, 100 kHz and 1 MHz at on oscillation level of 1 V. Microstructures of the fractured pellets were examined using scanning electron microscopy and average grain sizes were determined by a linear intercept method.

3. Results and discussion

Prepared B-site mixtures of the entire MN–ZN system were confirmed, by XRD analyses of Fig. 1a,

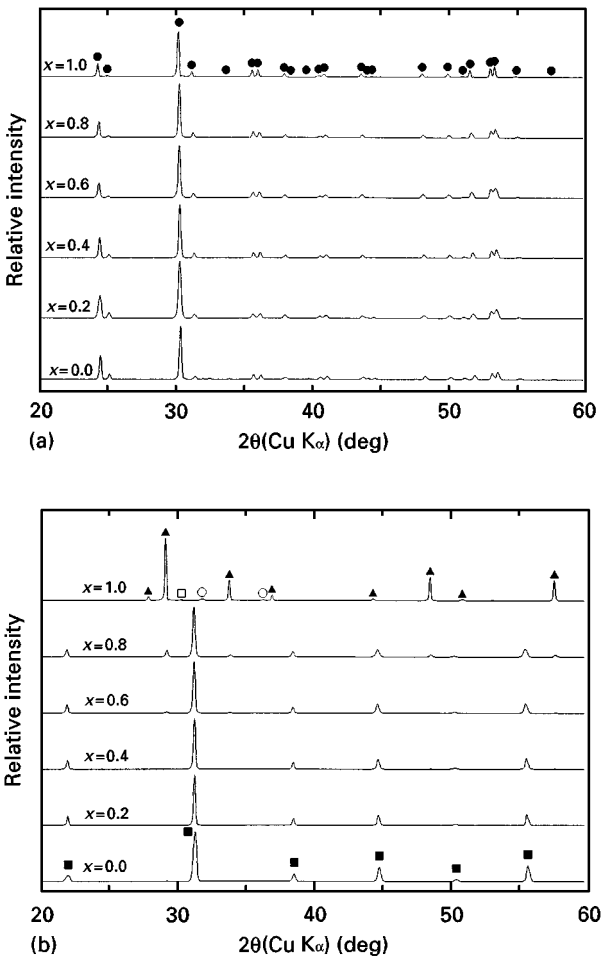

Figure 1 XRD spectra of (a) the B-site precursor $(1-x)$MN–xZN and (b) $(1-x)$PMN–xPZN powders. (●), columbite; (■), perovskite; (▲), pyrochlore; (□), PbO; (○), ZnO.

to form only the columbite phase. Since the two compounds, $MgNb_2O_6$ and $ZnNb_2O_6$, have the same crystal structure and the radii of the divalent Mg and Zn ions are nearly equal (0.72 versus 7.4 nm [12]), the crystalline solution of $Mg_{1-x}Zn_xNb_2O_6$ is readily formed as shown in Fig. 1a. In Fig. 1b are displayed the X-ray diffractograms of the system $(1-x)$PMN–xPZN, after a second calcination. For PMN, only a well-developed perovskite structure was observed. As Zn^{2+} replaced Mg^{2+}, a parasitic pyrochlore phase of $Pb_3Nb_4O_{13}$ [21] started to develop at $x = 0.6$. For $x > 0.6$, the pyrochlore phase gradually replaced the perovskite and finally became dominant in the extreme composition of PZN. For PZN, a complete pyrochlore phase, with trace amounts of PbO and ZnO, was detected. Therefore, preparation of PZN powders of perovskite structure was unsuccessful, as expected, and hereafter the PZN composition is not included in the $(1-x)$PMN–xPZN system for the rest of the study. As for the arrangement of B-site species, no superlattice peak was detected throughout the whole system (Fig. 1b), indicating an absence of ordering among the B-site cations.

In Fig. 2 are the perovskite contents, obtained by comparing perovskite (1 1 0) and pyrochlore (2 2 2) peak intensities, of the system powders after first and second calcinations, and of the sintered pellets. For PMN-rich compositions, nearly single-phase

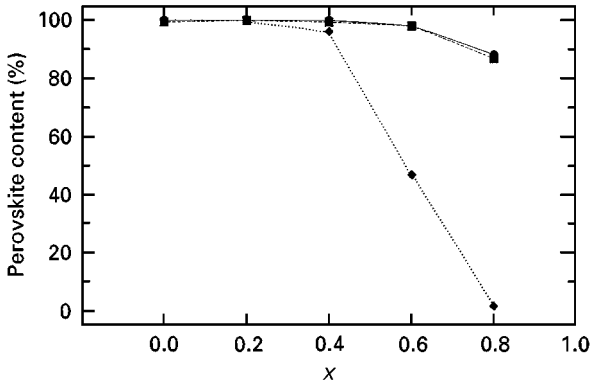

Figure 2 Variation of perovskite content in $(1-x)$PMN–xPZN powder, after first calcination (◆), after second calcination (■) and after sintering (●).

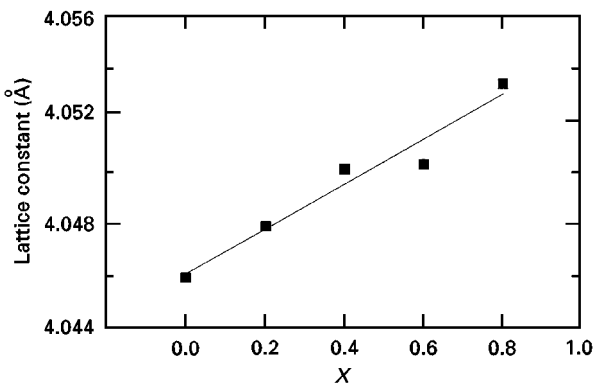

Figure 3 Lattice parameter versus x in the system $(1-x)$ PMN–xPZN.

perovskite powders were obtained after the first calcination and, as a result, the phase yield could not be increased by any significant amount by further heat treatments. For PZN-rich compositions, however, the double calcination definitely increased the yield, e.g., from 2% to 87% after the first and second calcinations for $x = 0.8$. Meanwhile these values of yield remained unchanged or increased only slightly after sintering. Overall perovskite contents after the sintering were 100% for $x = 0.0$–0.4, and 98% and 88% for $x = 0.6$ and $x = 0.8$, respectively. Lattice constants of the prepared powders were calculated from the data in Fig. 1b, assuming a pseudocubic structure and excluding the diffraction peaks corresponding to the pyrochlore phase, if any. The results are plotted in Fig. 3, where the overall tendency of gradual increase in the lattice parameter with replacement of Mg by Zn is quite obvious, considering the sizes of the Mg^{2+} (7.2 nm) and the Zn^{2+} (7.1 nm) ions [12]. The difference between the lattice parameters of PMN (40.46 nm) and PZN (40.55 nm, extrapolated value) is 0.009 nm, which is reasonable as only a third of the divalent cations (difference in radii, 0.2 nm) takes up positions in the perovskite unit cell. This consistency supports the validity of the reported ionic sizes (or at least the difference between them). The linear relation also demonstrates the formation of continuous solid solution up to $x = 0.8$ in the $(1-x)$PMN–xPZN relaxor system. The solubility limit seems to exist at $0.8 \leqslant x \leqslant 1.0$, as formation of the perovskite phase

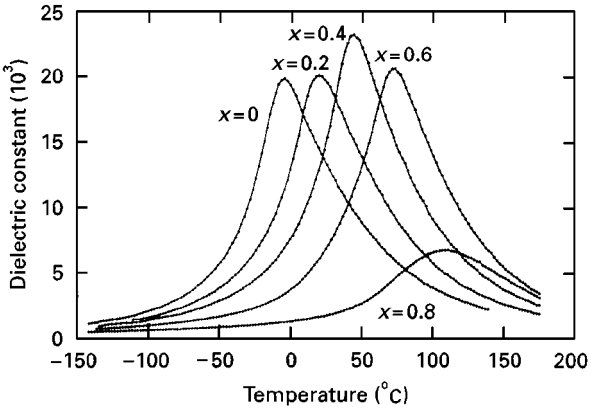

Figure 4 Temperature-dependent dielectric constants of $(1-x)$ PMN–xPZN ceramics (1 kHz).

was unsuccessful in the extreme composition of PZN. Geometrical densities of the sintered pellets were 93–97% of the theoretical values.

Fig. 4 shows the temperature-dependent dielectric constant spectra for the various compositions, measured at 1 kHz. With increasing Zn content, the Curie temperature, T_C, shifted towards high temperatures. In contrast, the maximum dielectric constant, K_{max}, reached a peak value of 23 000 for $x = 0.4$ and decreased at higher Zn contents. The dramatic decline to a value of 6800 at 110 °C for $x = 0.8$ is undoubtedly associated with the higher content (12%) of pyrochlore phase in the sample (Fig. 2). Dielectric loss–temperature characteristics were typical of the relaxor materials, the maximum loss and the peak temperature increased with increasing frequency. For PMN, the maximum value of dielectric loss was 13% at -20 °C. As the PZN content became higher, the maximum loss decreased while the peak temperature increased. The losses after the dielectric loss peak were about 0.1% throughout the system.

Dielectric constant–temperature characteristics of PMN and 0.2PMN–0.8PZN ceramics are shown in Fig. 5, where the Curie temperatures and maximum dielectric constants (1 kHz) were -5 °C and 110 °C, and 20 000 and 6800, respectively. Relaxation behaviours with DPT characters can clearly be observed for both compositions. The relaxation phenomenon reportedly originates from the disordered occupation of B-site components in the octahedra, which was verified by the absence of superlattice reflections in Fig. 1b. Dielectric spectra for $x = 0.2$–0.6 were similar to those in Fig. 5, with differences in only T_C and K_{max}.

In order to examine closely the relaxation behaviours and T_C shifts with composition change of the system, the composition- and frequency-dependent dielectric constant data were replotted as Fig. 6. With the composition change, the degree of relaxation became smaller, i.e., ΔT_C ($= T_{C,1\,MHz} - T_{C,1\,kHz}$) decreased from 17 to 15, 14, 10 and 4 °C as x changed from 0.0 to 0.8. Meanwhile, the T_C shifts with composition were almost linear and a monotonic increase in T_C with increasing PZN content also supports the solid solubility in the system PMN–PZN.

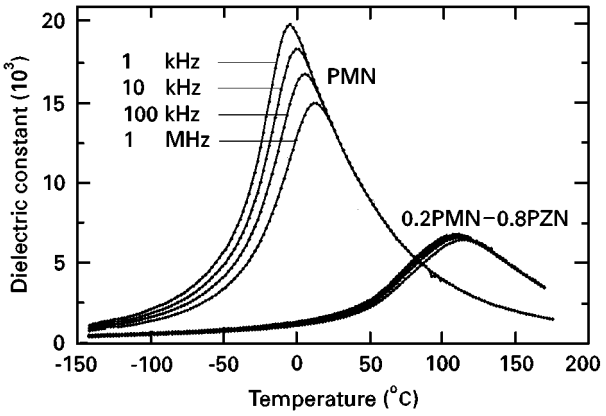

Figure 5 Dielectric relaxation phenomena in PMN and 0.2PMN–0.8PZN.

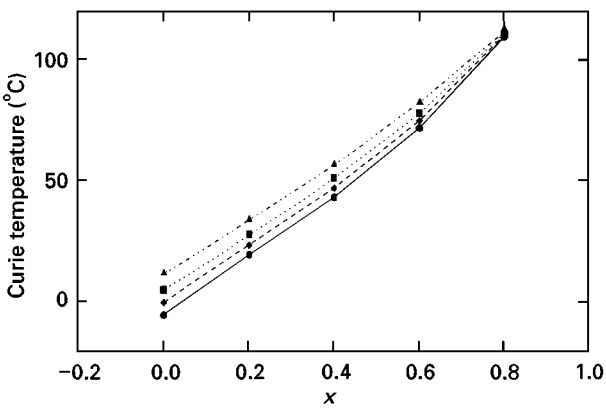

Figure 6 Composition- and frequency-dependent Curie temperatures of $(1-x)$PMN–xPZN ceramics. (▲), 1 MHz; (■), 100 kHz; (◆), 10 kHz; (●), 1 kHz.

It is widely accepted that the dielectric constants of relaxors in the paraelectric region cannot be expressed by the Curie–Weiss law of the first-order-type ferroelectric materials. Instead, they usually follow a quadratic relation [22] as follows:

$$\frac{1}{K} = \frac{1}{K_{\max}} + \frac{(T - T_C)^2}{2K_{\max}\delta^2}$$

where δ is a diffuseness coefficient, which indicates the degree of broadness (or diffuseness) of the dielectric constant peak. The value of δ can be obtained from the slope of a plot of $1/K$ versus $(T - T_C)^2$, which is shown in Fig. 7 for PMN measured at different frequencies. The curves were virtually straight and followed the quadratic rule quite closely. Using the slopes and appropriate $K_{\max}$ values, the diffuseness coefficients were calculated to be 37.0 K, 37.5 K, 38.1 K and 38.9 K at 1 kHz, 10 kHz, 100 kHz and 1 MHz, respectively, with a tendency to a monotonic increase in δ as the frequency increased. Meanwhile the values were 37.0, 36.3, 33.5, 33.2 and 43.5 K for $x = 0.0$–0.8 at 1 kHz, where δ decreased gradually as the PZN content increased (up to $x = 0.6$). The sudden increase to δ = 43.5 K ($x = 0.8$) can be attributed to the rather small value of $K_{\max}$ (Fig. 4) owing to the much higher pyrochlore content, compared with other compositions, which necessitates a subsequent increase in δ. For comparison, the diffuseness coefficient

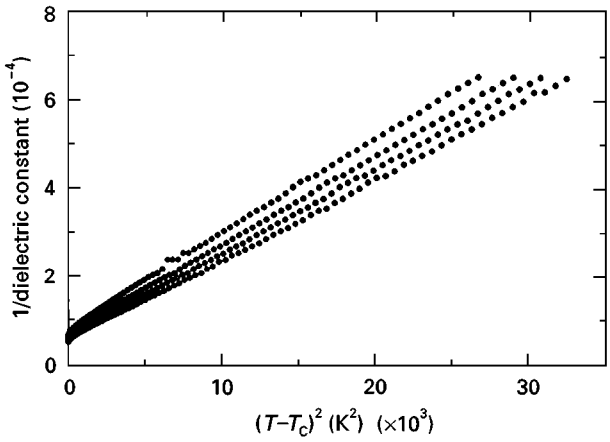

Figure 7 Reciprocal dielectric constant versus $(T - T_C)^2$ of PMN at different frequencies, with calculated diffuseness coefficients. From the top downwards, the data are for the frequencies 1 MHz (δ = 38.9 K), 100 kHz (δ = 38.1 K), 10 kHz (δ = 37.5 K) and 1 kHz (δ = 37.0 K).

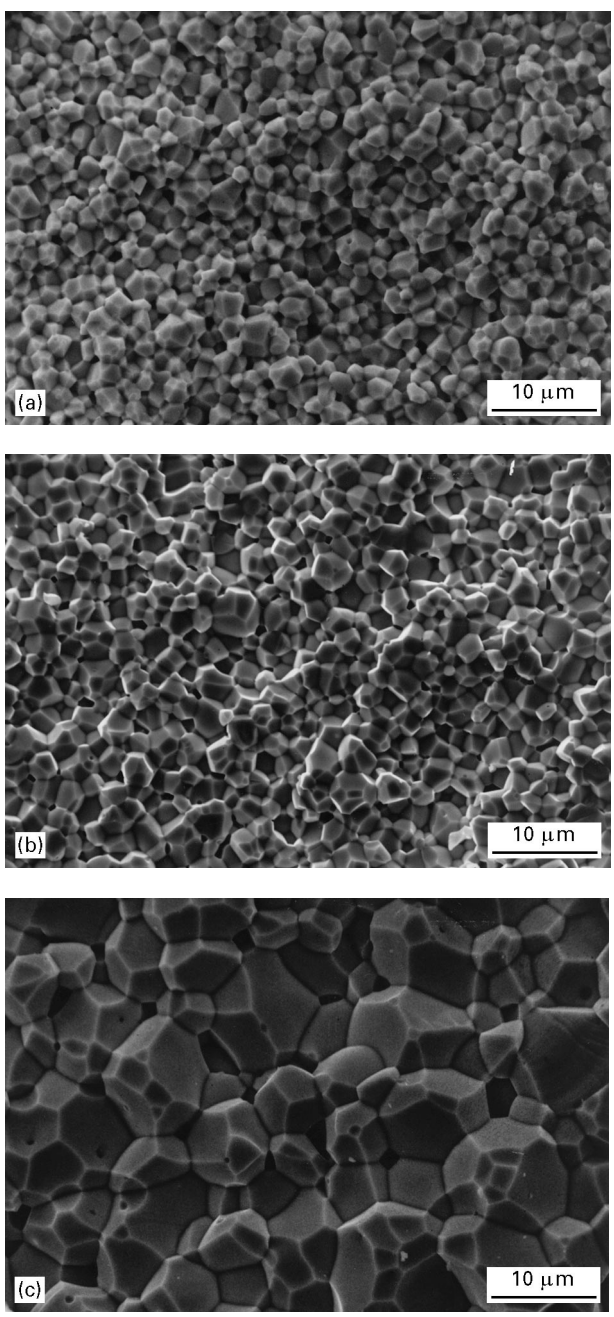

Figure 8 Microstructures of PMN ceramics, sintered at (1) 1150 °C, (b) 1200 °C and (c) 1250 °C for 1 h.

of $Pb(Mg_{1/3}Ta_{2/3})O_3$ [16] was 49 K, much larger than those of PMN–PZN ceramics, also owing to a small value of $K_{max} = 8700$.

Fig. 8 shows the microstructure development of PMN ceramics with increasing sintering temperature. The average grain sizes increased from 1.9 and 2.1 μm to 5.5 μm after sintering at 1150 and 1200 °C to 1250 °C, respectively. PMN pellets sintered at 1200 °C showed a maximum bulk density value and the density decreased after sintering at higher temperatures, which is due to rapid grain growth (occurring between 1200 and 1250 °C). Hence, 1200 °C was chosen as the optimum sintering condition for PMN ceramics and the temperatures for other compositions were selected likewise. For $x = 0.0$–0.4, typical microstructures of relaxor ferroelectric materials with uniformly sized and well-faceted grains were observable. For a 0.6PMN–0.4PZN composition, the microstructure was developed fully (with a grain size of 1.6 μm) after sintering at 1100 °C, and the specimen sintered at 1150 °C showed a slightly increased size of 2.1 μm. In Fig. 9 are scanning electron photomicrographs for $x = 0.6$ and $x = 0.8$. The well-faceted grains for $x = 0.0$–0.4 started to deform at $x = 0.6$ (Fig. 9a). From the phase analysis of Fig. 1b, a pyrochlore phase started to develop at $x = 0.6$, and this emergence of pyrochlore was evidenced in the microstructure as secondary phase grains. For $x = 0.8$ (Fig. 9b), small secondary grains were interspersed among the larger host grains and a great portion of the secondary phase caused the significant decrease in dielectric constant maximum in Fig. 4.

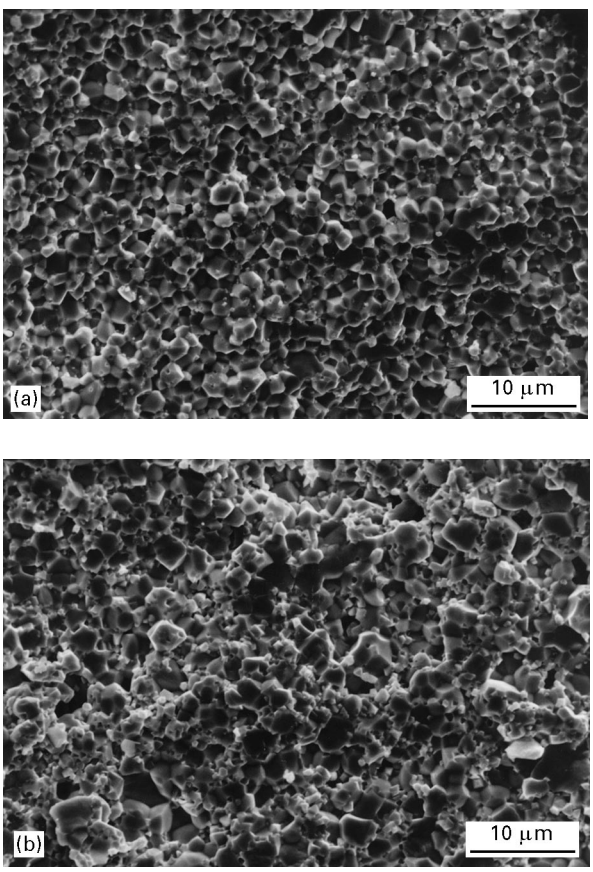

Figure 9 Microstructures for $(1 - x)$PMN–xPZN ceramics with (a) $x = 0.6$ and (b) $x = 0.8$.

4. Summary

A continuous crystalline solution of a columbite structure was prepared for $0.0 \leqslant x \leqslant 1.0$ in the B-site components of $Mg_{1-x}Zn_xNb_2O_6$. Calcined mixtures of PbO and the B-site precursors showed a well-developed perovskite structure for the PMN-rich composition ($0.0 \leqslant x \leqslant 0.6$ in $(1 - x)$PMN–xPZN), while a pyrochlore structure started to develop at $x = 0.6$. The development of a pyrochlore phase was also confirmed by the emergence of secondary grains in the microstructure. Lattice parameters of the perovskite structure in the PMN–PZN system showed a linear relationship and indicates a solid solubility, except for the composition PZN. The Curie temperatures and maximum dielectric constants (1 kHz) of PMN and 0.2PMN–0.8PZN were -5 °C and 110 °C, and 20 000 and 6800, respectively. The Curie temperature shifted monotonically towards high temperatures, with increasing Zn content, while the maximum dielectric constant reached a peak value of 23 000 for $x = 0.4$ and decreased at higher Zn contents. All the prepared ceramics showed typical relaxor behaviours, with the degree of relaxation decreasing as Zn gradually replaces Mg. The diffuseness coefficient increased with increasing frequency and decreased with increasing PZN content.

Acknowledgement

This work was supported by the Ministry of Education Research Fund for Advanced Materials during 1994–1997.

References

1. V. A. BOKOV and I. E. MYL'NIKOVA, *Sov. Phys.—Solid State* **3** (1961) 613.
2. G. SMOLENSKII, *Ferroelectrics* **53** (1984) 129.
3. N. SETTER and L. E. CROSS, *J. Mater. Sci.* **15** (1980) 2478.
4. I. G. ISMAILZADE, *Sov. Phys.—Crystallogr.* **5** (1960) 292.
5. Y. YAMASHITA, in Proceedings of the Seventh International Symposium on Applications of Ferroelectrics (IEEE, New York, 1990) p. 241.
6. *Idem., Amer. Ceram. Soc. Bull.* **73** (1994) 74.
7. V. A. BOKOV and I. E. MYL'NIKOVA, *Sov. Phys.—Solid State* **2** (1961) 2428.
8. S. TAKAHASHI, A. OCHI, M. YONEZAWA, T. YANO, T. HAMATSUKI and I. FUKUI, *Ferroelectrics* **50** (1983) 181.
9. S. J. JANG, K. UCHINO, S. NOMURA and L. E. CROSS, *ibid.* **27** (1980) 31.
10. K. UCHINO, *Amer. Ceram. Soc. Bull.* **65** (1986) 647.
11. R. E. WHATMORE, P. C. OSBOND and N. M. SHORROCKS, *Ferroelectrics* **76** (1987) 351.
12. R. D. SHANNON, *Acta Crystallogr. A* **32** (1976) 751.
13. Y. MATSUO, H. SASAKI, S. HAYAKAWA, F. KANAMARU and M. KOIZUMI, *J. Amer. Ceram. Soc.* **52** (1969) 516.
14. Y. YOKOMIZO and S. NOMURA, *J. Phys. Soc. Jpn, Suppl.* **28** (1970) 150.
15. Y. YOKOMIZO, T. TAKAHASHI and S. NOMURA, *ibid.* **28** (1970) 1278.

16. M.-C. CHAE and N.-K. KIM, *Ferroelectrics* (1997) in press.
17. B.-H. LEE, N.-K. KIM, B.-O. PARK and S.-H. CHO, *Mater. Lett.* **33** (1997) 57.
18. B.-H. LEE, N.-K. KIM, J.-J. KIM and S.-H. CHO, *Ferroelectrics* (1997) in press.
19. S. L. SWARTZ and T. R. SHROUT, *Mater. Res. Bull.* **17** (1982) 1245.
20. M.-C. CHAE, N.-K. KIM, J.-J. KIM and S.-H. CHO, *Ferroelectrics* (1997) submitted.
21. Joint Committee of Powder Diffraction Standards, "Powder diffraction file" (International Center for Diffraction Standards, Swarthmore, PA, 1991) Card 25-443.
22. V. V. KIRILLOV and V. A. ISUPOV, *Ferroelectrics* **5** (1973) 3.

Received 29 August 1996
and accepted 14 October 1997